

indicate a distribution of the presumptive auxin carriers part way up the sides of the cells in addition to the base would easily allow a lateral component to auxin transport if either only one side's carriers were activated or if basal and "other side" carriers were inhibited. Such differential activation of the auxin anion carriers is a concept already being incorporated into theoretical models of auxin transport in, for example, the geotropic response of stems (21).

The association of the labeled cells with vascular bundles in pea stems appears to be in general agreement with recent evidence from peas (6) that indicated a preferred auxin transport pathway within the vascular cylinder, specifically in cambium, procambium, and phloem initial cells. At this point, however, it is impossible for us to exclude the possibility that differential fluorescent labeling of cell and tissue types within our sections is due solely to such factors as differential penetration of cell walls by the immunoglobulin G antibody or a concentration of NPA binding sites in nonlabeled cells (or nonlabeled parts of basally labeled cells) that is too low to allow the development of a clear fluorescent signal. These alternatives deserve further investigation.

To our knowledge, this is the first report of monoclonal antibodies used to label plant tissue. Such antibodies are useful in that they can recognize a single antigenic site. Thus, one need not have a purified protein in order to obtain antibodies which specifically bind to it. We have obtained monoclonal antibodies that recognize an antigenic determinant of the NPA receptor in peas and have used them to identify that receptor at the basal ends of a population of pea stem parenchyma cells. In view of previous evidence linking NPA action to auxin efflux from cells and our present finding that the NPA binding site recognized by the monoclonal antibody used in our fluorescent localization studies can interact with auxin, these results strongly suggest that the auxin anion carrier of the chemiosmotic hypothesis is located at the basal plasma membrane of transporting cells.

MARK JACOBS
SCOTT F. GILBERT

Department of Biology,
Swarthmore College,
Swarthmore, Pennsylvania 19081

References and Notes

1. F. W. Went, *Rec. Trav. Bot. Neerl.* **25**, 1 (1928).
2. M. H. M. Goldsmith, *Annu. Rev. Plant Physiol.* **28**, 439 (1977).
3. G. Perbal, D. Driss-Ecole, Y. Leroux, *Physiol. Plant.* **56**, 285 (1982).
4. J.-L. Bonnemain, *C. R. Acad. Sci. Paris Ser. D* **273**, 1699 (1971).
5. E. Wangermann, *New Phytol.* **73**, 623 (1974).

6. D. A. Morris and A. G. Thomas, *J. Exp. Bot.* **29**, 147 (1978).
7. P. H. Rubery and A. R. Sheldrake, *Planta* **118**, 101 (1974).
8. J. A. Raven, *New Phytol.* **74**, 163 (1975).
9. M. H. M. Goldsmith, *Planta* **155**, 68 (1982).
10. _____ and P. M. Ray, *ibid.* **111**, 297 (1973).
11. G. Kohler and C. Milstein, *Nature (London)* **256**, 495 (1975).
12. C. A. Lembi, D. J. Morr , K. St.-Thomson, R. Hertel, *Planta* **99**, 37 (1971).
13. P. H. Rubery, *Annu. Rev. Plant Physiol.* **32**, 569 (1981).
14. M. R. Sussman and M. H. M. Goldsmith, *Planta* **151**, 15 (1981).
15. W. Z. Cande and P. M. Ray, *ibid.* **129**, 43 (1976).
16. M. R. Sussman and M. H. M. Goldsmith, *ibid.* **152**, 13 (1981).
17. M. R. Sussman and G. Gardner, *Plant Physiol.* **66**, 1074 (1980).
18. P. H. Quail, *Annu. Rev. Plant Physiol.* **30**, 425 (1979).
19. R. Hertel, in *Plant Organelles*, E. Reid, Ed. (Ellis Horwood, Chichester, 1979), p. 173.
20. M. Thom, W. M. Laetsch, A. Maretzki, *Plant Sci. Lett.* **5**, 245 (1975).
21. G. J. Mitchison, *Proc. R. Soc. London Ser. B* **214**, 69 (1981).
22. P. M. Ray, *Plant Physiol.* **59**, 594 (1977).
23. We thank G. Flickinger, P. Kloeckner, W. Kirby, and J. Halprin for technical assistance. Supported by grant PCM 81-04488 from the National Science Foundation (M.J.) and NIH grant HD-15032 (S.F.G.).

4 March 1983; revised 15 April 1983

Nuclear Transplantation in the Mouse Embryo by Microsurgery and Cell Fusion

Abstract. Nuclear transplantation in the mouse embryo was achieved by using a method that combines microsurgical removal of the zygote pronuclei with the introduction of a donor nucleus by a virus-mediated cell fusion technique. Survival of embryos was greater than 90 percent in tests of this procedure. The embryos developed to term at a frequency not significantly different from that of nonmanipulated control embryos. Because nuclei and cytoplasm from genetically distinct inbred mouse strains can be efficiently interchanged, this procedure may be useful in characterizing possible cytoplasmic contributions to the embryonic and adult phenotype.

Nuclear transplantation studies in the amphibian embryo have provided valuable information about the possible restriction of nuclear potential during development (1). Similar experiments in the mammalian embryo are hindered by the small size of the embryo and its sensitivity to microsurgical manipulation. Despite these obstacles, transplantation of donor nuclei obtained from inner cell mass cells was recently reported in the mouse embryo (2, 3). In those experiments, however, many of the manipulated embryos were lost because the plasma membrane was disrupted by a micropipette. We report a nuclear transplantation technique that avoids this loss by not requiring penetration of the embryo's plasma membrane with a micropipette. When pronuclei from a second one-cell stage embryo served as the nuclear donor, almost all embryos receiving this material survived the procedure and developed to term at a frequency comparable to that of unmanipulated control embryos.

Mouse embryos were incubated before and during microsurgery in cytochalasin B (2-5) and Colcemid. The embryo was secured by a holding pipette and the zona pellucida was penetrated with an enucleation pipette (Fig. 1). Penetration of the plasma membrane was avoided and the pipette was advanced into the embryo at a point adjacent to a pronucleus. Upon aspiration, a small portion of ovum plasma membrane and surrounding cytoplasm was drawn into the pipette, followed by the pronucleus. The pipette, now containing an entire pronucleus, was then moved to a point adjacent to the second pronucleus and the latter was similarly aspirated. As the enucleation pipette was withdrawn, a cytoplasmic bridge could be seen extending from the pronuclei in the pipette to the embryo (Fig. 1A). With continued withdrawal of the pipette, this bridge stretched to a fine thread and pinched off (Fig. 1B). The pipette, which now contained the membrane-bound pronuclei (pronuclear karyoplast), was moved to a

Table 1. Efficiency of the nuclear transplantation technique.

Genotype	Enucleation*	Karyoplast injection†	Fusion‡
C3H/HeJ	24 of 26	24 of 24	23 of 24
C57BL/6J	35 of 35	34 of 35	34 of 34
ICR	11 of 12	10 of 11	10 of 10
Total (%)	70 of 73 (96)	68 of 70 (97)	67 of 68 (99)

*Number of embryos surviving microsurgical removal of both the male and female pronuclei per total number of embryos. †Number of pronuclear karyoplasts surviving injection into the perivitelline space of the recipient embryo per total number of karyoplasts injected. ‡Number of pronuclear karyoplasts fusing with the recipient embryo per total number of karyoplast-injected embryos.

second drop containing Sendai virus inactivated with β -propiolactone (2000 to 3000 hemagglutinating units per milliliter), and a small volume of virus suspension, approximately equal to the volume of the pronuclear karyoplast in the pipette, was aspirated. The pipette was then moved to a third drop containing a previously enucleated embryo. The zona pellucida of this embryo was penetrated at the previous site of enucleation, and the virus suspension and pronuclear karyoplast were injected sequentially into the perivitelline space (Fig. 1C) (6). The pipette was withdrawn and the embryo was incubated at 37°C. Fusion of the pronuclear karyoplast with the enucleated embryo usually occurred during the first hour of incubation (Fig. 1D).

Thus, with this procedure, it is possible to transfer the nuclei from one embryo to another without penetrating the plasma membrane. Furthermore, it becomes possible to use large-bore pipettes, which are necessary to accommodate pronuclei but are highly disruptive in existing mechanical microinjection techniques.

To determine the overall efficiency of this transplantation procedure and its effects on subsequent development, we transplanted pronuclei between genetically distinct one-celled mouse embryos and transferred to the uteri of pseudopregnant females those embryos that had developed to the blastocyst stage after 5 days in vitro. Control embryos isolated at the one-cell stage were similarly cultured and transferred to the uteri of pseudopregnant females, but were not exposed to cytoskeletal inhibitors or inactivated Sendai virus. Of 73 experimental embryos, 70 (96 percent) were successfully enucleated, and of the 70 pronuclear karyoplasts obtained, 68 (97 percent) were successfully introduced (with Sendai virus) into the perivitelline space of enucleated zygotes (Table 1). After incubation at 37°C, 67 (99 percent) of these karyoplasts fused to the plasma membrane of the ovum. The overall efficiency of nuclear transplantation was therefore 91 percent.

After microsurgery, experimental and control embryos were cultured for 5 days and the number of embryos successfully developing to the blastocyst stage was determined. Of 34 control embryos, all developed to the morula or blastocyst stage (Table 2). Similarly, of the 67 experimental embryos, 64 (96 percent) developed to the morula or blastocyst stage. Transfer of the 34 control embryos to the uteri of pseudopregnant females resulted in the birth of five progeny (15 percent), three of which survived to adulthood. Transfer of the 64 experimen-

tal embryos to the uteri of pseudopregnant females resulted in the birth of ten progeny (16 percent), seven of which survived to adulthood. These seven offspring all displayed the coat color phenotype of the donor nuclei, and five were fertile.

Thus the technical manipulations in-

volved in transferring pronuclei from one zygote to another did not significantly affect the ability of embryos to undergo normal development. The high frequency of developmental arrest in both the experimental and control groups after the implantation procedure may have resulted from the in vitro culture period

Table 2. Development of control and nuclear-transplant embryos. The subscripts N and C refer to the strain origin of the nucleus and of the cytoplasm, respectively.

Group and strain	Developmental stage by day 5 in vitro (number of embryos)			Number born*
	Arrested	Morula	Blastocyst	
Control				
C3H/HeJ	0	3	11	0
C57BL/6J	0	1	13	4
ICR	0	1	5	1
Total	0	5	29	5
Nuclear-transplant				
C3H/He _N to C57BL/6J _C	0	0	23	4
C57BL/6J _N to C3H/He _C	0	1	23	3
ICR _N to C57BL/6J _C	1	0	9	2
C57BL/6J _N to ICR _C	2	0	8	1
Total	3	1	63	10

*Number of offspring born after transfer of morulae and blastocysts into the uteri of females in the third day of pseudopregnancy.

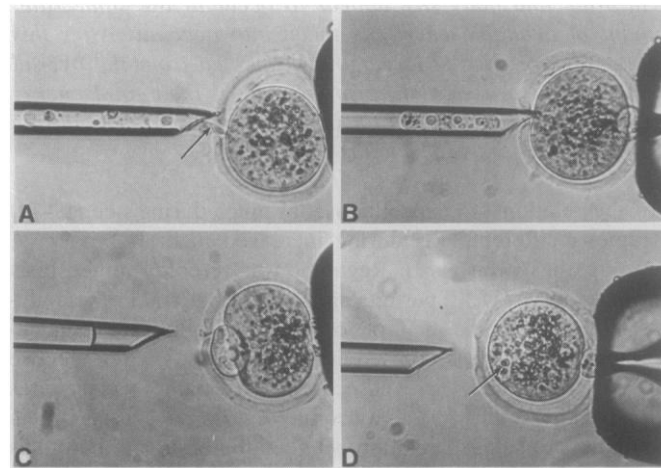


Fig. 1. Nuclear transplantation in the mouse embryo. One-cell stage embryos were obtained from oviducts excised from spontaneously mated females on the day of vaginal plug detection (day 1). Cumulus cells were dispersed in Whitten medium (8) containing bovine hyaluronidase (500 non-filtered units per milliliter). The embryos were washed four times and cultured to the blastocyst stage in 50- μ l drops of modified Whitten medium (9) under silicone oil at 37°C in an atmosphere of 5 percent O₂, 5 percent CO₂, and 90 percent N₂ (10). Medium containing cytochalasin B (5 μ g/ml) and Colcemid (0.1 μ g/ml) was prepared weekly, stored at 4°C, and protected from light. Microsurgery was performed with Leitz micromanipulators and a fixed-stage Leitz Laborlux II microscope. Holding and enucleation pipettes were fashioned from Pyrex capillary tubing (outer diameter, 1.0 mm; inner diameter, 0.65 mm). For holding pipettes (outer diameter, 75 to 100 μ m), the capillary tubing was hand-pulled over a microburner, placed on a DeFonbrune microforge, broken on a glass anvil, and polished. Enucleation pipettes (outer diameter, 15 to 20 μ m) were fashioned with a DKI 200 vertical pipette puller and their tips were beveled on a grinding wheel, dissolved in a solution of hydrofluoric acid (25 percent), and sharpened on a microforge. They were then treated with 100 percent Nonidet P40, rinsed thoroughly, and stored overnight. Before microsurgery, groups of six to eight embryos were incubated for 15 to 45 minutes at 37°C in an atmosphere of 5 percent O₂, 5 percent CO₂, and 90 percent N₂ in bicarbonate-buffered Whitten medium containing cytochalasin B and Colcemid. They were then placed singly in hanging drops of Hepes-buffered Whitten medium containing cytochalasin B (5 μ g/ml) and Colcemid (0.1 μ g/ml) in a Leitz oil chamber. Microsurgery was performed as described in text, and the embryos were washed and returned to the incubator. All microsurgery was performed at room temperature. Sendai virus was obtained from the infected allantoic fluid of embryonated chicken eggs and inactivated with β -propiolactone (11-13). (A) Light micrograph of an embryo in the process of enucleation. Note the pronuclei in the pipette and the cytoplasmic bridge (arrow) between the cytoplasm of the embryo and the pronuclear karyoplast. (B) Light micrograph of an enucleated embryo. The pipette contains the pronuclei surrounded by a small volume of cytoplasm and a portion of the embryo's plasma membrane. (C) Light micrograph of an enucleated embryo after introduction of inactivated Sendai virus and the pronuclear karyoplast into the perivitelline space. (D) Light micrograph of an embryo shortly after fusion of the pronuclear karyoplast to the enucleated embryo. Note the peripheral location of the pronuclei (arrow).

tal embryos were washed and returned to the incubator. All microsurgery was performed at room temperature. Sendai virus was obtained from the infected allantoic fluid of embryonated chicken eggs and inactivated with β -propiolactone (11-13). (A) Light micrograph of an embryo in the process of enucleation. Note the pronuclei in the pipette and the cytoplasmic bridge (arrow) between the cytoplasm of the embryo and the pronuclear karyoplast. (B) Light micrograph of an enucleated embryo. The pipette contains the pronuclei surrounded by a small volume of cytoplasm and a portion of the embryo's plasma membrane. (C) Light micrograph of an enucleated embryo after introduction of inactivated Sendai virus and the pronuclear karyoplast into the perivitelline space. (D) Light micrograph of an embryo shortly after fusion of the pronuclear karyoplast to the enucleated embryo. Note the peripheral location of the pronuclei (arrow).

before implantation, since the intrauterine transfer of 22 carrier blastocysts that had developed in vivo resulted in the birth of 17 progeny. The method described here can also be used to introduce donor nuclei obtained from later-stage embryonic cells into enucleated zygotes (7). This procedure may therefore aid in further defining the possible developmental restriction of nuclei during mammalian embryogenesis. In addition, reciprocal pronuclear transplantations between genetically distinct one-celled embryos may be used to define the degree to which maternally inherited cytoplasmic components persist.

JAMES MCGRATH
DAVOR SOLTER

Wistar Institute of
Anatomy and Biology,
Philadelphia, Pennsylvania 19104

References and Notes

1. J. F. Danielli and M. DiBerardino, *Int. Rev. Cytol. Suppl.* 9 (1979).
2. K. Illmensee and P. C. Hoppe, *Cell* 23, 9 (1981).
3. P. C. Hoppe and K. Illmensee, *Proc. Natl. Acad. Sci. U.S.A.* 79, 1912 (1982).
4. ———, *ibid.* 74, 5657 (1977).
5. J. A. Modlinski, *J. Embryol. Exp. Morphol.* 60, 153 (1980).
6. T. P. Lin, J. Florence, J. O. Oh, *Nature (London)* 242, 47 (1973).
7. J. McGrath and D. Solter, unpublished results.
8. W. K. Whitten, *Adv. Biosci.* 6, 129 (1971).
9. J. Abramczuk, D. Solter, H. Koprowski, *Dev. Biol.* 61, 378 (1977).
10. J. McGrath and N. Hillman, *Nature (London)* 283, 479 (1980).
11. R. E. Giles and F. H. Ruddle, *In Vitro* 9, 103 (1973).
12. J. M. Neff and J. F. Enders, *Proc. Soc. Exp. Biol. Med.* 127, 260 (1968).
13. C. F. Graham, *Acta Endocrinol. Suppl.* 153, 154 (1971).
14. Supported by grants CA-10815, CA-25875, and CA-27932 from the National Cancer Institute, by grant HD-12487 from the National Institute of Child Health and Human Development, and by grant PCM-81 18801 from the National Science Foundation. J.M. was supported by NCI grant T32-CA-09171.

16 December 1982; revised 29 March 1983

Relative Brain Size and Metabolism in Mammals

Abstract. Comparisons of the relation between brain and body weights among extant mammals show that brain sizes have not increased as much as body sizes. Interspecific increases in brain and body size appear to occur at the same rate, however, when the amount of available energy is taken into account. After this adjustment, brains of primates are slightly larger than expected from the overall mammalian data, but primates also use a larger proportion of their total energy reserves for their brains. Analyses of relative brain size must take into account the requirements that the metabolically active brain has for the body.

For the past 50 years the relation of brain to body weights among different mammalian taxonomic groups has been thought to scale allometrically at 0.67 (1, 2), but recent expansion of the data base led to estimates of the slope being approximately 0.75 (3). The newer and larger sets of points may have disproportionately increased the numbers of small mammals with relatively small brains and this alone could produce a steeper slope (4). Although the reason for the discrepancy between the slopes is not known, the mammalian data sets appear regular and contain certain consistent deviations; anthropoids (1–3, 5), pinnipeds, and odontocetes (5) are highly encephalized and frugivorous bats are more encephalized than insectivorous ones (6), a situation that may have parallels among primates (7).

The causal factors controlling brain to body-weight scaling are not known, but it has been conjectured that the scaling reflects the functions of the brain for analyzing sensory information and controlling motor output (2, 8). The brain controls the body's actions but also needs the body for its energy supply. The brain is metabolically very active and demands a large supply of oxygen

and glucose, as much during sleep (9–11) as during increased mental activity (9, 11). Regulation of cerebral homeostasis permits small perturbations in the delivery of oxygen and glucose, but decreased availability of oxygen or glucose are associated with pathological states such as coma (9, 10, 12). The metabolic relation between the brain and body has received attention (3, 13, 14), but its role in relative brain size has not been adequately analyzed (15). It is proposed here that the size of the brain will be constrained both by the size of the system delivering oxygen and glucose and by the rate at which energy can be expended on supporting the brain's constantly high metabolic demands. Body weight is a first approximation of the size of the storage and delivery systems for glucose and oxygen, and the organism's basal (standard) metabolic rate (BMR) estimates the amount of available oxygen and energy per unit time (16).

In this study brain weights of 93 adult mammalian species were collected from the literature (1–3, 6, 13, 17) and analyzed allometrically in terms of both body weight and body mass times the metabolic rate. These adjusted body weights parallel the animal's caloric ex-

penditure. Only species that had brain weights, body weights, and BMR's (in cubic centimeters of O₂ per 100 g per minute) were used. If the studies in which the species-specific brain weight and BMR were determined used individuals of a species whose body weights differed by more than 10 percent, the BMR was adjusted (13). Rates of total brain metabolism measured with the Kety-Schmidt technique were also taken from the literature (13). Linear regressions and principal axes were used to study the relation among the logarithmically transformed data. Comparisons of intercepts or adjusted group means are based on analyses of covariance ($N - 3$ degrees of freedom) and reported as t -tests (Table 1).

The overall picture of the regression of brain weights against body weights resembles other mouse-to-elephant curves (Fig. 1). The relation is best described by the linear regression equation $\log E = -1.28 + 0.76 \log S$ [$r = .976$, 95 percent confidence limits of the slope (cls) = 0.743 to 0.779], where E = brain weight and S = body weight; (slope of the principal axis = 0.761). The slope from these data is very close to recent estimates (3) and higher than the 0.67 slopes reported earlier (1, 2, 5). Although primates ($\log E = -1.11 + 0.81 \log S$; 95 percent cls = 0.693 to 0.927; $r = .973$) have larger relative brains compared to all other mammals ($\log E = -1.29 + 0.74 \log S$; 95 percent cls = 0.707 to 0.776; $r = .983$), the pinnipeds and odontocetes have relatively big brains with values overlapping those of large anthropoids (18). Furthermore, the pinnipeds and odontocetes have larger relative brain sizes than do terrestrial ungulates (artiodactyls, perissodactyls, and elephant). Frugivorous bats have bigger brains per body weight (19) than insectivorous bats, corroborating earlier reports (6, 7) (Table 1). Because only one insectivorous primate, *Galago demidovii* (20), was included in this sample, statistical analyses were not run on dietary differences among primates.

For this mammalian sample, the amount of O₂ consumed per body weight is described by the equation $\log \text{BMR} = 0.84 - 0.269 \log S$ (95 percent cls = -0.292 to -0.248 ; $r = -.93$; principal axis slope = -0.270), and the slope is close to the predicted -0.25 one (21). The unexplained variance for BMR to body weight is higher than that for brain to body weight, reflecting either an increase in measurement error or a larger biological variation. Several taxonomic deviations from the overall trend occur here too. Primates ($\log \text{BMR} = 0.60 -$